IntensityEnhanced Apodization Effect on an Axially Illuminated Circular Column ParticleLens

Yue, Liyang; Yan, Bing; Monks, James; Dhama, Rakesh; Wang, Zengbo; Minin, Oleg; Minin, Igor

Annalen der Physik

Published: 01/02/2018

Peer reviewed version

Intensity-enhanced apodization effect on an axially illuminated circular-column particle-lens

Liyang Yue[1], Bing Yan[1], James N. Monks[1], Rakesh Dhama[1], Zengbo Wang[1], Oleg V. Minin[2], and Igor V. Minin[3]

[1]School of Electronic Engineering, Bangor University, Bangor, LL57 1UT, UK
[2]National Research Tomsk State University, Lenin Ave., 36, Tomsk, 634050, Russia
[3]National Research Tomsk Polytechnic University, Lenin Ave., 30, Tomsk, 634050, Russia

Corresponding authors E-mails: l.yue@bangor.ac.uk and prof.minin@gmail.com

Abstract
A particle can function as a refractive lens to focus a plane wave, generating a narrow, high intensive, weak-diverging beam within a sub-wavelength volume, known as the 'photonic nanojet'. It is known that apodization method, in the form of an amplitude pupil-mask centrally situated on a particle-lens, can further reduce the waist of a photonic nanojet, however, it usually lowers the intensity at the focus due to blocking the incident light. In this paper, the anomalously intensity-enhanced apodization effect was discovered for the first time via numerical simulation of focusing of the axially illuminated circular-column particle-lenses, and a greater than 100% peak intensity increase was realised for the produced photonic nanojets.

Short title: L. Yue, B. Yan, J. N. Monks, R. Dhama, Z. Wang, O. V. Minin, and I. V. Minin: Intensity-enhanced apodization effect

Key words: Apodization; particle-lens; diffraction; scattering; near-field optics;

A photonic nanojet is a localised high-intensity focusing area near the shadow surface of the dielectric particle-lens illuminated by a plane wave. Refractive index contrast (particle to background media) and scaling effect of the dielectric particle (relative-to-wavelength size) play key roles in photonic nanojet formation, rather than the shape of particle-lens [1, 2]. Waist determined by the full width at half maximum (FWHM) of a photonic nanojet could be smaller than the diffraction limit which defines the minimum distance between two objects to be imaged as two instead of one [3, 4]. Many important applications for imaging and sensing, e.g. super-resolution microscopy, tight-focusing laser scalpels, exotic waveguide, and high-resolution coherent anti-Stokes Raman scattering microscopy, have been afforded based upon the super-resolution characteristic of the photonic nanojet [5-11]. This has led researchers around the world to attempt to further reduce this waist with a variety of methods [1]. In geometrical optics, focusing the radiation in the least possible space requires an increase in the contribution of rays passing through the aperture of lens periphery. Amplitude apodization of lens aperture can be accomplished by adding a super-resolution annular mask in lens system to inhibit the diffraction edge effect and increase the numerical aperture (NA) of the lens [12]. This far-field super-resolution element may have been firstly studied by Toraldo di francia et al. in 1952, and an accurately tailored sub-wavelength diffraction spot was obtained with the suggestion of a pupil design in their work [13]. Nevertheless, central screening of an aperture caused by the amplitude mask normally results in intensity loss at the focus [14, 15]. Thus, mask apodization is thought to be a method that should only be adapted in a situation when optical energy efficiency is sufficient [16, 17].

Minin et al. and Yan et al. independently discovered that mask apodization not only applies to the far-field system, but also functions in the near-field range and effectively shortens the waist of a photonic nanojet by a spherical or cuboid particle-lens despite intensity loss [18-20]. However, we found the anomalously intensity-enhanced near-field apodization effect on the axially illuminated circular-column particle-lenses via numerical simulation in this study, which is able to simultaneously provide the extra intensity enhancement and waist shortage to the produced photonic nanojet. Focusing of a

circular-column particle-lens illuminated from the flat end was firstly investigated to demonstrate this phenomenon against a variety of particle-lens scales in comparison with that for spherical particle-lenses. Radial illumination of the particles with the same shapes has been studied in the previous literatures [21, 22]. More than 100% growth of maximum E^2 field intensity can be achieved for the photonic nanojet by an apodized circular-column model with the particular dimension.

Current models are built in the commercial finite integral technique software package – CST Microwave Studio©. A plane wave of 1064 nm wavelength (λ), which is polarised along y axis, propagates from $+z$ to $-z$ direction. All apodized models are structured as a fused silica circular-column or sphere particle-lens covered by an aluminium pupil-mask. While, the same sized non-masked models are also established as references. Optical properties - refractive index, n, and extinction coefficient, k, for fused silica ($n = 1.45$, $k = 0.5 \times 10^{-5}$) and aluminium ($n = 1.22$, $k = 10.42$) are based on the previous literatures [23, 24]. A certain length, L, normalised to λ is assigned to all dimensions in this approach, as shown in insets of Fig. 1. Diameter of the simulated pupil-masks are $L/2$.

Fig. 1 (a-d) illustrate the distributions of E^2 field intensity in xz plane for the spherical and circular-column particle-lenses models both in the size of $L = 3\lambda$ with and without the mask apodizations. In Fig. 1 (a) and (b) for the models of the spherical particle-lens, both photonic nanojets are formed at the lower boundary of the particle-lens and elongate into the background medium. It is shown that maximum E^2 field intensity of non-pupil-masked spherical model is higher than that for the pupil-masked model (34.9/33.6), which is in accordance with our previous study regarding the intensity sacrifice in apodization for the spherical particle-lens [19]. Subsequently, mask apodization significantly benefits the growth of the maximum E^2 field intensity in models of the axially illuminated circular-column particle-lens, as shown in Fig. 1 (c) and (d). Fig. 1 (d) manifests that two wave flows circumvent the pupil-mask to enter the particle-lens from the side, then converge at the bottom and form a short but high-intensity photonic nanojet, aided by the internal refraction. In this process, mask apodization makes E^2 field intensity of the photonic nanojet produced by the circular-column particle-lens maximise to 42.3, which is more than twice as high as 20.5 realised by the corresponding non-pupil-masked model.
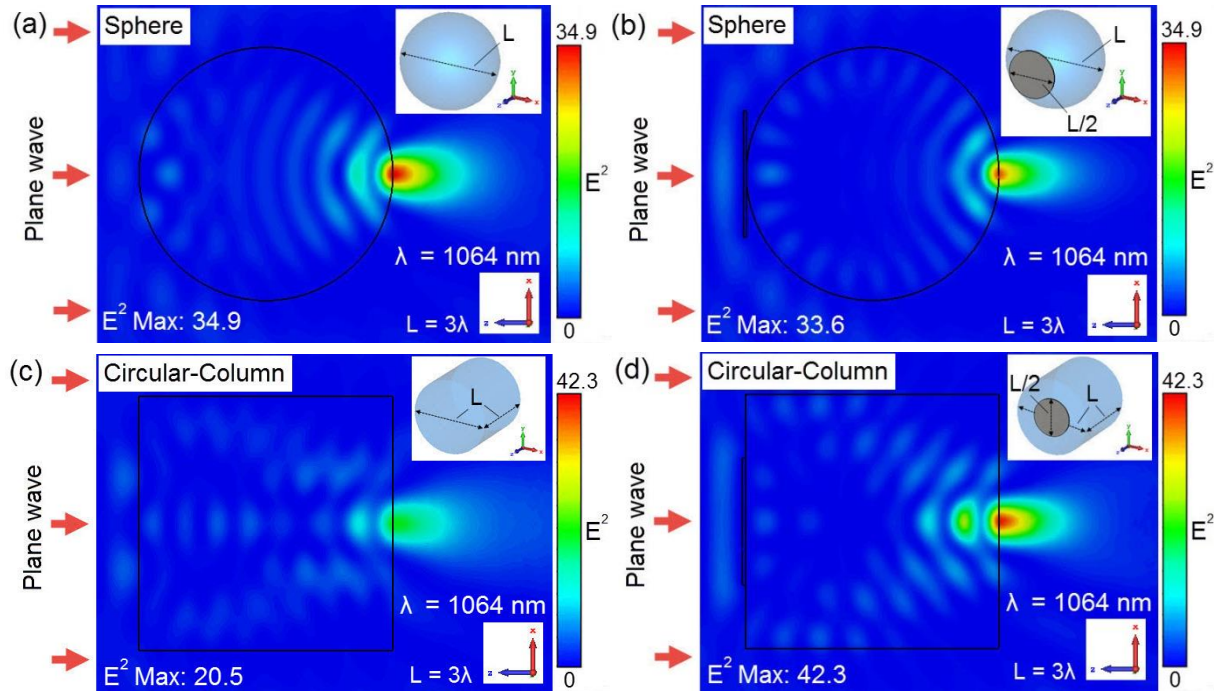

Figure 1 E^2 field intensity distribution in xz plane for the particle-lenses in the shapes of sphere (a), (b) and the axially illuminated circular-column (c), (d) with/without the mask apodization.

Fig. 2 exhibits statistics of maximum E^2 field intensities and FWHMs for models with two shapes, where dimensions are ranged from $L/\lambda = 1$ to 3, and data is collected every 0.25 to investigate the scaling behaviours of the aforementioned intensity-enhanced apodization effect. In the first row, it is shown that models of the non-pupil-masked spherical particle-lens provide higher maximum E^2 field intensity

(black curve) than that for the pupil-masked model (red curve) in the whole scaling range. Maximum E^2 field intensity (red curve) constantly increases with the size growth of the axially illuminated circular-column particle-lens with mask apodization, and is almost larger than that for the non-pupil-masked model (black curve) at every scale except $L/\lambda = 1$, as shown in the second row of Fig. 2. A significant promotion of more than 100% raise of maximum E^2 field intensity (red curve) is achieved at $L/\lambda = 3$ through mask apodization (black dashed line in Fig. 2). This peak value - 42.3 is 18.9% larger than that for the same-size spherical model without mask apodization.

The third and fourth rows of Fig. 2 summarise the normalised FWHM/λ for the spherical and circular-column models with and without mask apodization. Positions of the focuses along the z axis where FWHMs are calculated are z = -3209 nm, -3180 nm, -3210 nm, and -3190 nm for the models of non-masked sphere, masked sphere, non-masked circular-column, and masked circular-column, respectively, which means FWHMs of two masked models are measured inside the particle-lens with $L = 3\lambda$ that occupies the space between z = 0 nm and z = -3192 nm. Diffraction limit in the particle-lenses $-\lambda/2n$ and diffraction limit in the air $-\lambda/2$ are displayed as benchmarks (black dashed lines) in these two rows. Generally, mask apodization in the form of an amplitude pupil-mask on the particle effectively reduces the waists of photonic nanojets in all models within the simulated scale range in Fig. 2. Thus, the third row of Fig. 2 shows that only photonic nanojets induced by the pupil-masked spherical particle-lens can be beyond the diffraction limit in the particle-lens - $\lambda/2n$ in the scale range of $1.25 < L/\lambda < 3$, but the diffraction limit in the air - $\lambda/2$ can be usually overcome by the axially illuminated circular-column particle-lens models with the mask apodization, as shown in the fourth row of Fig. 2. Besides, it is noted that FWHM/λ achieved in the model of an apodized circular-column particle-lenses is almost constant in our simulated dimensional range.
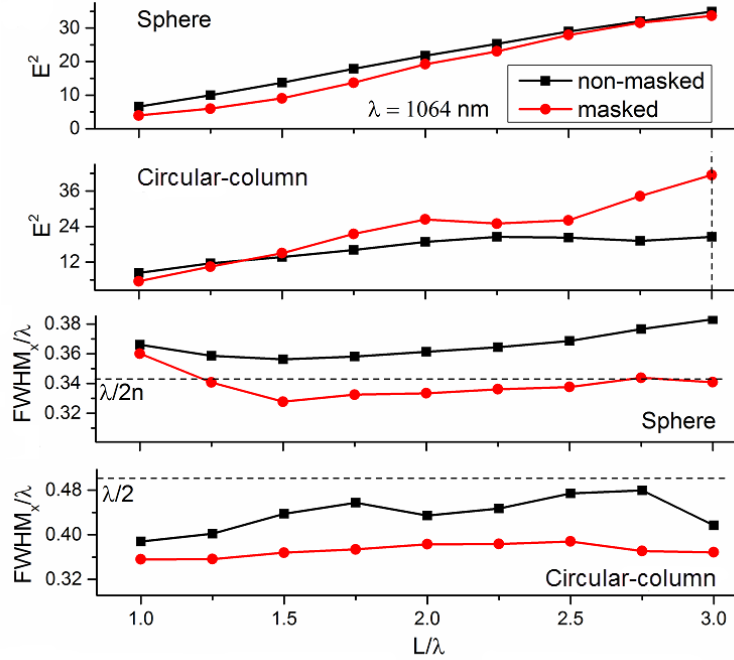

Figure 2 Statistics of maximum E^2 field intensities and FWHM/λ for the models of the spherical and circular-column particle-lenses ranged from $L/\lambda = 1$ to 3 with and without the mask apodization.

Fig. 1 and 2 show that circular-column is an ideal shape for particle-lens to stimulate the axially intensity-enhanced apodization effect in this study. To explore the formation mechanism, power flow diagrams in xz plane are plotted in Fig. 3 (a) and (b) for the $L = 3\lambda$ non-pupil-masked and pupil-masked circular-column models, respectively. In Fig. 3 (a), three power flows (light blue colour) enter the non-pupil-masked circular-column particle from the upper boundary (left side), then converge into a photonic nanojet (yellow colour) at the lower boundary (right side). By contrast, only two wider but more high-intensity power flows split by the pupil-mask input into the particle-lens after the mask apodization, as shown in Fig. 3 (b). The formed photonic nanojet (dark red colour) possesses higher intensity and smaller waist compared to those in non-pupil-masked model (Fig. 3 (a)). In Fig. 3 (b), the input areas where power flows enter the particle almost extend to the middle of the cross-section (red

3

circle in Fig. 3 (b)) due to the diffraction caused by the amplitude mask, which guides more power flows to the sides. The same areas for the non-pupil-masked model in Fig. 3 (a) are much smaller, only covering the corners (red circle in Fig. 3 (a)).

Also, many vortices of power flow are found in the flank of the non-pupil-masked circular-column, as shown in Fig. 3 (a). Vortices established within the power flow diagrams suggest the stable focuses in the phase space [25]. Power flow couples to the other planes through the singular points at the centre of the vortex [26], which normally reduces amount of wave energy in a single plane. Therefore, larger input area allows convergence of more power flows, leading to fewer vortexes in flank. These are considered as the two main factors to cause the intensity-enhanced apodization effect for the axially illuminated circular-column particles. In fact, it is known that formation of a photonic nanojet in a non-spherical particle-lens is due to the phase delay along the wave front caused by diffraction [27], which cannot be simply described using refraction in geometrical optics as for the spherical or conical particle-lenses [2, 27]. In our case, mask apodization increases the NA of the circular-column particle-lens and moves focus toward to its lower boundary, which is a phenomenal analogy to increase of refractive index of particle-lens material. It could be another reason to lead the intensity-enhanced apodization effect on that particle-lens shape. Power flow diagrams of the spherical models are shown in Figure S1 in the supplement, and the aforementioned major factors to increase the intensity of the photonic jet, especially extension of the input area of power flows, are not exhibited in it.
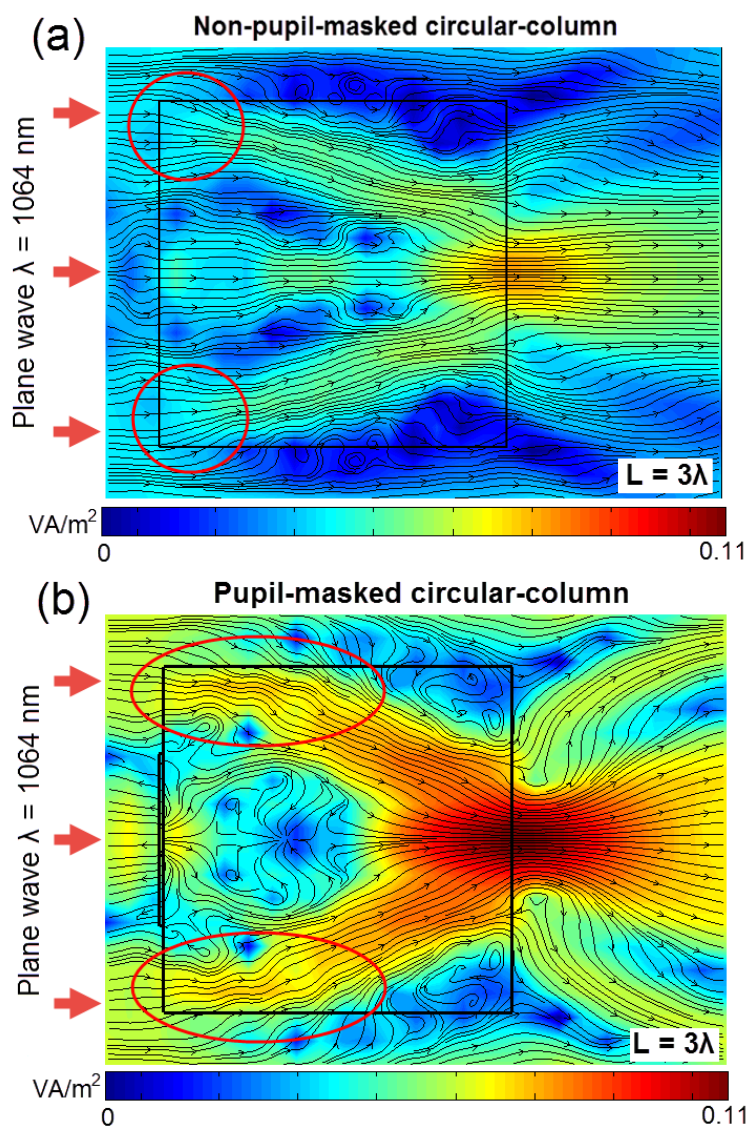

Figure 3 Power flow diagrams for the $L = 3\lambda$ circular-column particle-lens model without (a) and with (b) the mask apodization.

In conclusion, the intensity-enhanced apodization effect was firstly discovered in simulation of focusing of an axially illuminated circular-column particle-lens. It is able to simultaneously provide the extra intensity enhancement and waist shortage to the produced photonic nanojet, and increase of maximum E^2 field intensity can be over 100%. Convergence of power flows and analogy of increase of effective refractive index for the particle-lens material could be the reasons for the corresponding phenomenon. This finding is important and meaningful in the applications of imaging and sensing.

References
[1] B.S. Luk'yanchuk, R. Paniagua-Dominguez, I. Minin, O. Mini, and Z. B. Wang, Opt. Mater. Express **7**, 1820-1847 (2017).
[2] I. V. Minin, and Oleg V. Minin, Diffractive Optics and Nanophotonics: Resolution Below the Diffraction Limit (Springer, 2016).
[3] B. Yan, Z. B. Wang, A. L. Parker, Y. Lai, P. J. Thomas, L. Yue, and J. N. Monks, Appl. Opt. **56**, 3142-3147 (2017).
[4] F. A. Jenkins, and H. E. White, *Fundamentals of Optics, 3rd ed.* (McGraw-Hill Primis Custom Publishing, 1951).
[5] Z. B. Wang, Nanoscience **3**, 193-210 (2016).
[6] I. Alessandri, and J. R. Lombardi, Chem. Rev. **116**, 14921–14981 (2016).
[7] Z. B. Wang, W. Guo, L. Li, B. Luk'yanchuk, A. Khan, Z. Liu, Z. Chen, and M. Hong, Nat. Commun. **2**, 218 (2011).
[8] K. W. Allen, N. Farahi, Y. Li, N. I. Limberopoulos, D. E. Walker, A. M. Urbas, V. Liberman, and V. N. Astratov, Ann. Phys. (Berl.) **527**, 513-522 (2015).
[9] V. N. Astratov, A. Darafsheh, M. D. Kerr, K. W. Allen, N. M. Fried, A. N. Antoszyk, and H. S. Ying, SPIE Newsroom **12**, 32-34 (2010).
[10] K. W. Allen, A. Darafsheh, F. Abolmaali, N. Mojaverian, N. I. Limberopoulos, A. Lupu, and V. N. Astratov, Appl. Phys. Lett. **105**, 021112 (2014).
[11] P. K. Upputuri, Z. Wu, L. Gong, C. K. Ong, and H. Wang, Opt. Express 22, 12890-12899 (2014).
[12] H. Wang, C. J. R. Sheppard, K. Ravi, S. T. Ho, and G. Vienne, Laser Photonics Rev. **6**, 354–392 (2012).
[13] G. Toraldo di Francia, Nuovo Cimento **9**, 426 – 438 (1952).
[14] J. Ojeda-Castaneda, E. Tepichin, and A. Pons, Appl. Opt. **27**, 5140-5145 (1988).
[15] C. J. R. Sheppard, and A. Choudhury, Appl. Opt. **43**, 4322-4327 (2004).
[16] H. Luo, and C. Zhou, Appl. Opt. **43**, 6242-6247 (2004).
[17] M. Yun, M. Wang, and L. Liu, J. Opt. A: Pure Appl. Opt. **7**, 640 (2005).
[18] I. V. Minin, and O. V. Minin, Patent of Russia N 153686 (2015).
[19] B. Yan, L. Yue, and Z. B. Wang, Opt. Commun. **370**, 140–144 (2016).
[20] L. Yue, B. Yan, J. N. Monks, Z. B. Wang, N. T. Tung, V. D. Lam, O. Minin, and I. Minin, J. Phys. D: Appl. Phys. **50**, 175102 (2017).
[21] Z. Chen, A. Taflove, and V. Backman, Opt. Express **12**, 1214–1220 (2004).
[22] C. M. Ruiz, and J. J. Simpson, Opt. Express **18**, 16805– 16812 (2010).
[23] I. H. Malitson, J. Opt. Soc. Am. **55**, 1205-1208 (1965).
[24] E. D. Palik, *Handbook of Optical Constants of Solids, vol. 1*. (Academic Press, 1985).
[25] N. V. Karlov, N. A. Kirchenko, and B. S. Luk'yanchuk, Laser Thermochemistry: Fundamentals and Applications (Cambridge International Science, 2000).
[26] Z. B. Wang, B. S. Luk'yanchuk, M. H. Hong, Y. Lin, and T. C. Chong, Phys. Rev. B **70**, 035418 (2004).
[27] I. V. Minin, O. V. Minin, and Y. Geintz, Ann. Phys. (Berlin) **527**, 491 (2015).